

Supporting Information

Hydrophilic interaction chromatography coupled to ultraviolet photodissociation affords identification, localization, and relative quantitation of glycans on intact glycoproteins

Virginia K. James,¹ Annika A.M. van der Zon,^{2,3} Edwin E. Escobar,¹ Sean D. Dunham,¹ Andrea F. G. Gargano,^{2,3} Jennifer S. Brodbelt^{1*}

1. Department of Chemistry, University of Texas at Austin, Austin, TX 78712
2. van 't Hoff Institute for Molecular Science, University of Amsterdam, Science Park 904, 1098 XH Amsterdam, The Netherlands
3. Centre of Analytical Sciences Amsterdam, Science Park 904, 1098 XH Amsterdam, The Netherlands

*Correspondence to: jbrodbelt@cm.utexas.edu

Table S1. Protein sequences, masses and catalog numbers	S3
Table S2. 40 min HILIC gradient	S4
Table S3. 60 min HILIC gradient	S5
Table S4. 90 min HILIC gradient	S6
Table S5. PLRP gradient	S7
Table S6. Average intact mass of RNase B glycoforms	S8
Table S7. Tables of identified fragment ions from MS2 experiments and relative quantitation of RNase B, HA, and the RBDs	Excel spreadsheet
Table S8. Relative abundances of RNase B glycoforms compared to literature values	S9
Table S9. Average intact mass of HA glycoforms	S10
Table S10. Relative abundances of HA glycoforms	S11
Table S11. Average intact masses of RBD (WT and variants)	S12
Table S12. Relative abundances of RBD (WT and variants) O-linked glycoforms compared to literature values	S13
Figure S1. PLRP vs HILIC separations for RNase B	S14
Figure S2. ESI mass spectra and deconvoluted mass spectra obtained for RNase B	S15
Figure S3. Sequence maps based on HCD, ETD, ETHcD, and UVPD of RNase B	S16
Figure S4. UVPD spectrum of RNase B and a few fragment identifications	S17

Figure S5. Comparison of chromatographic peak shapes for MS1 only vs UVPD run	S18
Figure S6. Relative abundance of RNase B glycoforms	S19
Figure S7. ESI mass spectrum of HA collected via direct infusion	S20
Figure S8. EICs and corresponding ESI mass spectra for each glycoform of HA	S21
Figure S9. Sequence coverage maps of additional HA glycoforms derived from UVPD	S22
Figure S10. UVPD spectrum of a tryptic peptide that confirms the N terminal modification of the WT RBD	S23
Figure S11. Sequence maps of each O-glycoform of WT RBD based on UVPD	S24
Figure S12. Full range and deconvoluted MS1 spectra of WT RBD	S25
Figure S13. (a) EICs for the most abundant charge states of each O-glycoform of K417N/E484K/N501Y RBD, and (b) MS1 spectra corresponding to the retention time at the peak maximum.	S26
Figure S14. (a) EICs for the most abundant charge states of each L452R RBD O-glycoform, and (b) MS1 spectra corresponding to the retention time at the peak maximum.	S27
Figure S15. (a) EICs for the most abundant charge states of each G476S RBD O-glycoform, and (b) MS1 spectra corresponding to the retention time at the peak maximum.	S28
Figure S16. (a) EICs for the most abundant charge states of each A475V RBD O-glycoform, and (b) MS1 spectra corresponding to the retention time at the peak maximum.	S29
Figure S17. (a) EICs for the most abundant charge states of each E484K RBD O-glycoform, and (b) MS1 spectra corresponding to the retention time at the peak maximum.	S30
Figure S18. Sequence maps of each O-glycoform of K417N/E484K/N501Y RBD based on UVPD	S31
Figure S19. Sequence maps of each O-glycoform of L452R RBD based on UVPD	S32
Figure S20. Sequence maps of each O-glycoform of G476S RBD based on UVPD	S33
Figure S21. Sequence maps of each O-glycoform of A475VRBD based on UVPD	S34
Figure S22. Sequence maps of each O-glycoform of E484K RBD based on UVPD	S35

Table S1. Protein sequences and monoisotopic masses^a

Name	Sequence	Modification sites	Theoretical monoisotopic mass (without glycans)	Source
RNase B	KETAAAKFERQHMDSTSAASSSNYCNQMMKSRNLTKDRCKPVNTFVHESLADVQAVCSQKNVACKNGQTNCYQSYSTMSITDCRETGSSKYPNCAYKTTQANKHIIIVACEGNPYVPVHFDAVS	N: N34 O: none	13,681.32 Da	New England Biolabs P7817S
Partial length Hemagglutinin A (HA) (57-267 aa)	APHLGKCNIAAGWILGNPECESLSTASSWSYIVETPSSDNGTCYPGDFIDYEELREQLSSVSSFERFEIFPKTSSWPNHDSNKGVTAACPHAGAKSFYKNLIWLKKGNSYPKLSKSYINDKGKEVLVLWGIHPSTADQQSLYQNADTYVFGSSRYSKKFKPEIAIRPKV RDQEGRMNYWTLVEPGDKITFEATGNLVVPRYAFAMERNAGSGHHHHHHHH	N: unknown O: none	25,390.47 Da	Georgiou lab (UT-Austin)
WT RBD	QRVQPTESIVRFPNITNLCPFGEVFNATRFASVYAWNRKRISNCVADYSVLYNSASFSTFKCYGVSPTKLNLCFTNVYADSFVIRGDEVQRQIAPGQTGKIADYNYKLPDDFTGCVIAWNSNNLDSKVGGNYNLYRFLFRKSNLKPFRDISTEIQAGSTPCNGVEGFNCYFPLQSYGFQPTNGVGYQPYRVVLSFELLHAPATVCGPKKSTNLVKNKCVNFHHHHHH	N: N14, N26 O: T6 -NH ₃ N term	26,033.77 Da	BEI resources NR-52946
RBD L452R	RVQPTESIVRFPNITNLCPFGEVFNATRFASVYAWNRKRISNCVADYSVLYNSASFSTFKCYGVSPTKLNLCFTNVYADSFVIRGDEVQRQIAPGQTGKIADYNYKLPDDFTGCVIAWNSNNLDSKVGGNYNLYRFLFRKSNLKPFRDISTEIQAGSTPCNGVEGFNCYFPLQSYGFQPTNGVGYQPYRVVLSFELLHAPATVCGPKKSTNLVKNKGGGSGGGSHHHHHHHHH	N: N13, N25 O: T5	26,548.99 Da	BEI resources NR-55403
RBD G476S	RVQPTESIVRFPNITNLCPFGEVFNATRFASVYAWNRKRISNCVADYSVLYNSASFSTFKCYGVSPTKLNLCFTNVYADSFVIRGDEVQRQIAPGQTGKIADYNYKLPDDFTGCVIAWNSNNLDSKVGGNYNLYRFLFRKSNLKPFRDISTEIQASSTPCNGVEGFNCYFPLQSYGFQPTNGVGYQPYRVVLSFELLHAPATVCGPKKSTNLVKNKCVNFGGGSGGGSHHHHHHHHH	N: N13, N25 O: T5	26,999.17 Da	BEI resources NR-55401
RBD K417N/E484K/N501Y	RVQPTESIVRFPNITNLCPFGEVFNATRFASVYAWNRKRISNCVADYSVLYNSASFSTFKCYGVSPTKLNLCFTNVYADSFVIRGDEVQRQIAPGQTGNIADYNYKLPDDFTGCVIAWNSNNLDSKVGGNYNLYRFLFRKSNLKPFRDISTEIQAGSTPCNGVKGFNCFYPLQSYGFQPTYGVGYQPYRVVLSFELLHAPATVCGPKKSTNLVKNKGGGSGGGSHHHHHHHHH	N: N13, N25 O: T5	26,539.99 Da	BEI resources NR-55414
RBD A475V	RVQPTESIVRFPNITNLCPFGEVFNATRFASVYAWNRKRISNCVADYSVLYNSASFSTFKCYGVSPTKLNLCFTNVYADSFVIRGDEVQRQIAPGQTGKIADYNYKLPDDFTGCVIAWNSNNLDSKVGGNYNLYRFLFRKSNLKPFRDISTEIQVGSTPCNGVEGFNCYFPLQSYGFQPTNGVGYQPYRVVLSFELLHAPATVCGPKKSTNLVKNKGGGSGGGSHHHHHHHHH	N: N13, N25 O: T5	26,534.00 Da	BEI resources NR-55402
RBD E484K	RVQPTESIVRFPNITNLCPFGEVFNATRFASVYAWNRKRISNCVADYSVLYNSASFSTFKCYGVSPTKLNLCFTNVYADSFVIRGDEVQRQIAPGQTGKIADYNYKLPDDFTGCVIAWNSNNLDSKVGGNYNLYRFLFRKSNLKPFRDISTEIQAGSTPCNGVKGFNCFYPLQSYGFQPTNGVGYQPYRVVLSFELLHAPATVCGPKKSTNLVKNKGGGSGGGSHHHHHHHHH	N: N13, N25 O: T5	26,505.02 Da	BEI resources NR-55400

a. Point substitution numbers represent the amino acid number of the full length SARS-CoV-2 spike protein. The receptor binding domain (RBD) corresponds to residues 319-537 of the full length spike protein.

Table S2. HILIC gradient (40 minutes) used for RNase B runs.^a

Time (min)	%B
0	94
3	94
5	85
30	50
31	20
32	85
33	20
34	94
40	94

a. Analytical mobile phases consisted of (A) 98% water and 2% acetonitrile, (B) 98% acetonitrile and 2% water both with 0.1% formic acid and 0.05% TFA

Table S3. HILIC gradient (60 minutes) used for RBD quantitation, HA quantitation, and HA UVPD runs.^a

Time (min)	%B
0	94
3	94
5	85
50	50
51	20
52	85
53	20
54	94
60	94

a. Analytical mobile phases consisted of (A) 98% water and 2% acetonitrile, (B) 98% acetonitrile and 2% water both with 0.1% formic acid and 0.05% TFA

Table S4. HILIC gradient (90 minutes) used for RBD UVPD runs. ^a

Time (min)	%B
0	94
3	94
5	85
80	50
81	20
82	85
83	20
84	94
90	94

a. Analytical mobile phases consisted of (A) 98% water and 2% acetonitrile, (B) 98% acetonitrile and 2% water both with 0.1% formic acid and 0.05% TFA

Table S5. PLRP gradient^a

Time (min)	%B
0	2
5	2
7	8
40	35
41	90
45	90
46	2
60	2

a. Analytical mobile phases consisted of (A) 98% water and 2% acetonitrile, (B) 98% acetonitrile and 2% water both with 0.1% formic acid

Table S6. Average intact mass of RNase B glycoforms

Glycan	Average mass (Da)
5 mannose	14,907
6 mannose	15,069
7 mannose	15,231
8 mannose	15,393

Table S7. Tables of identified fragment ions from MS2 experiments and relative quantitation of RNase B, HA, and the RBDs.

(see Excel spreadsheet)

Table S8. Relative abundances of RNase B glycoforms compared to reported values

Glycoform	Relative abundance (%), this study (intact proteins)	Relative abundance (%), from Ref. 1 (proteolysis method)
5 mannose	54 ± 1	48
6 mannose	36 ± 1	33
7 mannose	6 ± 0	7
8 mannose	4 ± 1	9

(1) Hua, S.; Nwosu, C. C.; Strum, J. S.; Seipert, R. R.; An, H. J.; Zivkovic, A. M.; German, J. B.; Lebrilla, C. B. Site-Specific Protein Glycosylation Analysis with Glycan Isomer Differentiation. *Anal Bioanal Chem* **2012**, 403 (5), 1291–1302. <https://doi.org/10.1007/s00216-011-5109-x>.

Table S9. Average intact mass of HA glycoforms

Glycan	Average mass (Da)
deglycosylated	25,406
H3N4F1	26,851
H5N2	26,623
H5N4F1S1	27,467
H3N5F1	27,054
H4N4F1	27,013
H4N5F1	27,216
H5N4F1	27,175

Table S10. Relative abundances of HA glycoforms

Glycan	peak area %
deglycosylated	17.1 ± 1.2
H3N4F1	12.8 ± 1.9
H5N2	9.2 ± 0.4
H5N4F1S1	25.2 ± 1.9
H3N5F1	7.3 ± 0.1
H4N4F1	9.4 ± 0.7
H4N5F1	9.3 ± 1.7
H5N4F1	9.7 ± 0.8

Table S11. Average intact masses of RBD (WT and variants) O-linked glycoforms

	H1S1N1	H1S2N1	H2S1N2	H2S2N2
WT	26,690 Da	26,981 Da	27,056 Da	27,347 Da
L452R	27,294 Da	27,586 Da	N/A	27,952 Da
K417N/E484K/N501Y	27,286 Da	27,577 Da	N/A	27,942 Da
G476S	27,745 Da	28,036 Da	N/A	28,035 Da
A475V	27,279 Da	27,571 Da	N/A	27,936 Da
E484K	N/A	27,542 Da	N/A	27,907 Da

Table S12. Relative abundances of RBD (WT and variants) O-linked glycoforms compared to values reported in Ref. 1

	H1S1N1	H1S2N1	H2S1N2	H2S2N2
WT	14.4 ± 1	38.5 ± 2	22.2 ± 0	24.9 ± 2
L452R	8.3 ± 1	73.8 ± 3	N/A	16.9 ± 2
K417N/E484K/N501Y	9.8 ± 0	73.7 ± 1	N/A	17.2 ± 2
G476S	11.4 ± 1	75.2 ± 2	N/A	13.1 ± 1
A475V	12.4 ± 1	72.7 ± 1	N/A	15.2 ± 2
E484K	N/A	77.7 ± 0	N/A	22.9 ± 1
WT from Ref 1^a	2.2	65.4	6.5	10.0

a. Three other acetylated glycoforms were also identified with abundances ranging from 2.8% to 5.4%.

1. Roberts, D. S.; Mann, M.; Melby, J. A.; Larson, E. J.; Zhu, Y.; Brasier, A. R.; Jin, S.; Ge, Y. Structural O-Glycoform Heterogeneity of the SARS-CoV-2 Spike Protein Receptor-Binding Domain Revealed by Top-Down Mass Spectrometry. *J. Am. Chem. Soc.* **2021**, *143* (31), 12014–12024. <https://doi.org/10.1021/jacs.1c02713>.

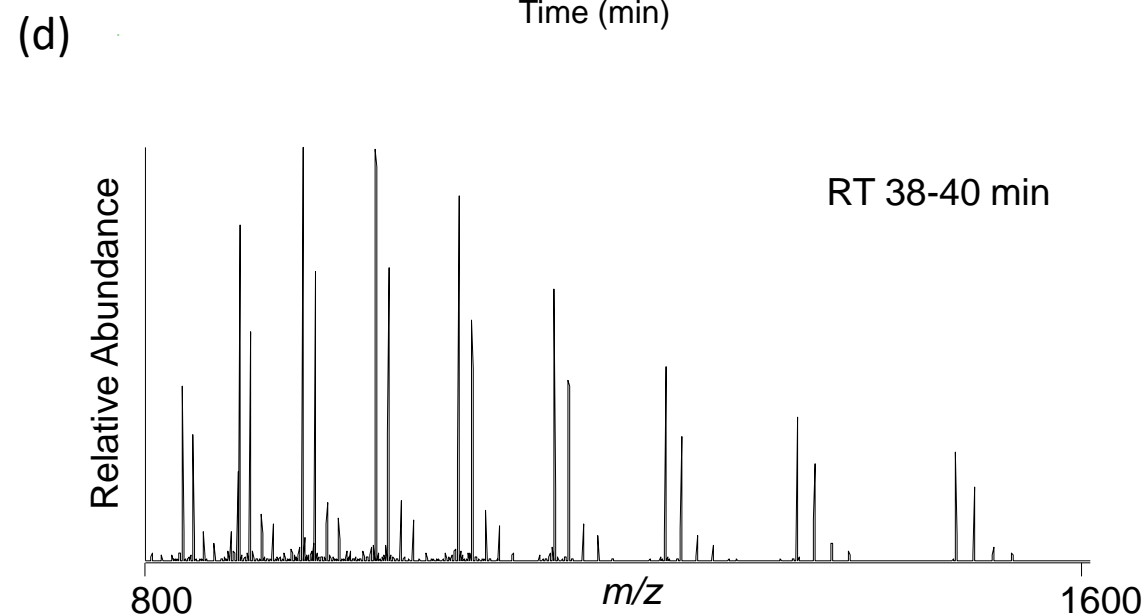
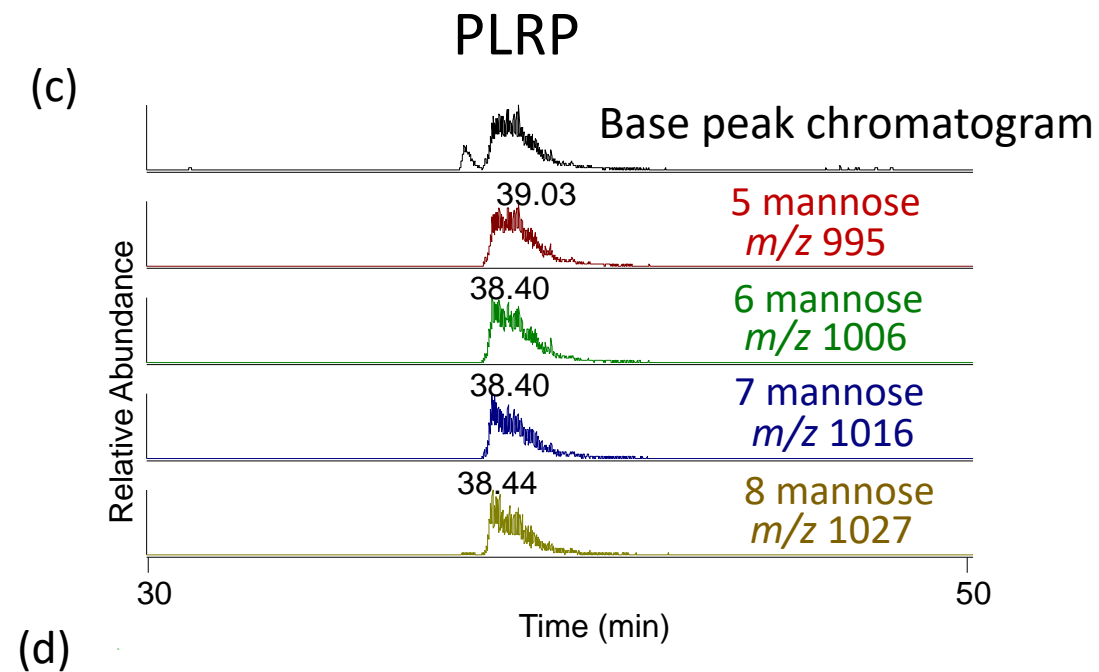
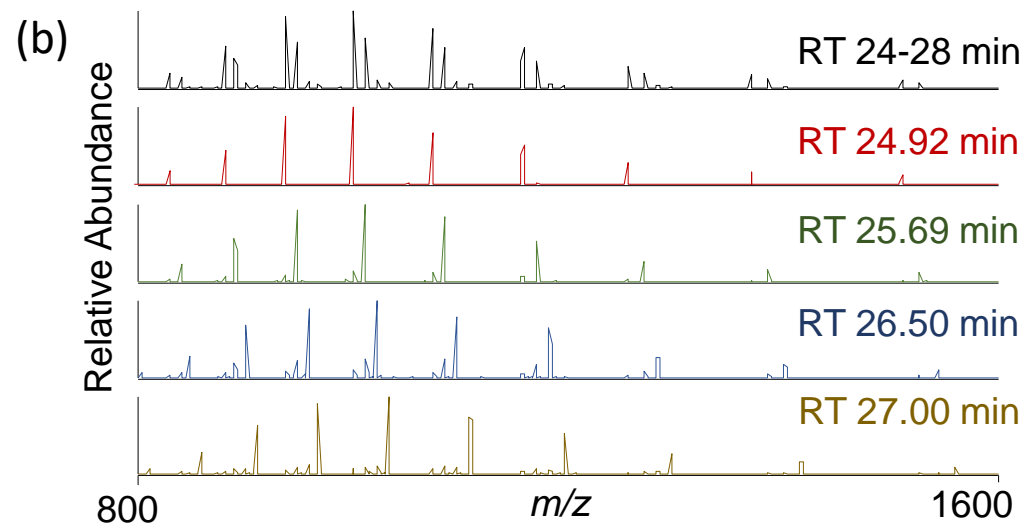
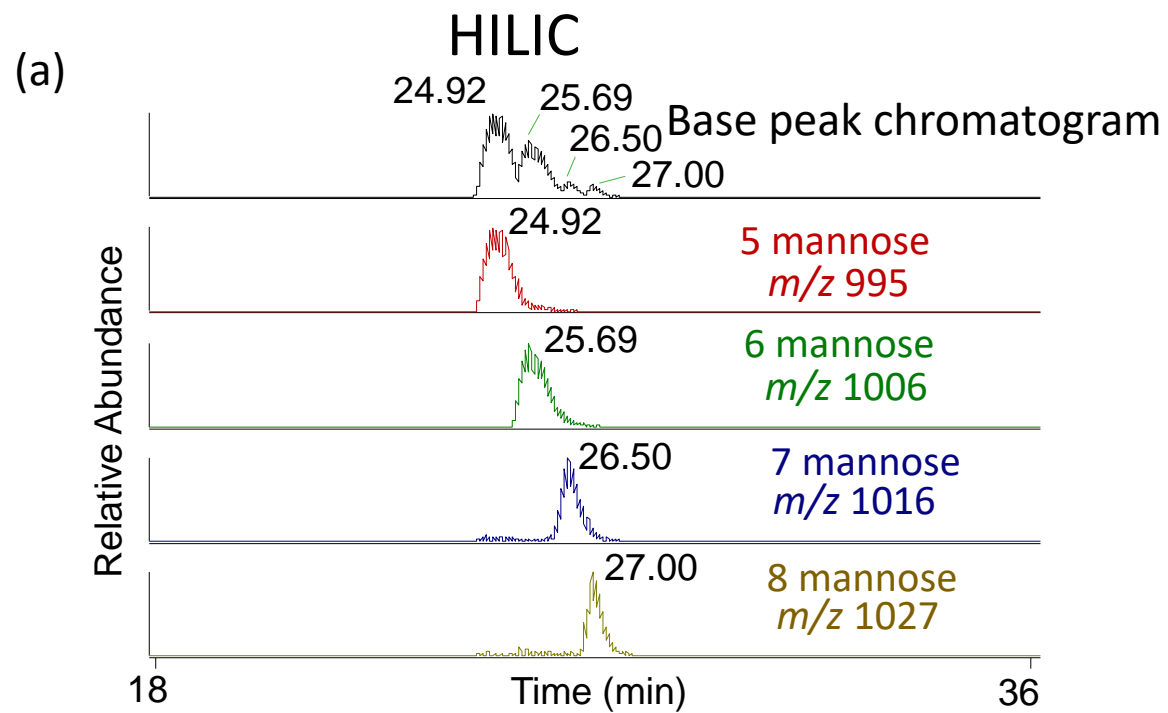


Figure S1. (a) Base peak (upper trace) and four EIC chromatograms obtained using HILIC of RNase B and (b) mass spectra to facilitate comparisons between HILIC and PRLP runs. (c) Base peak (upper trace) and four EIC chromatograms obtained using reversed phase (PLRP) separation of RNase B, and (d) corresponding mass spectrum corresponding to the unresolved chromatographic peak at 38-40 min.

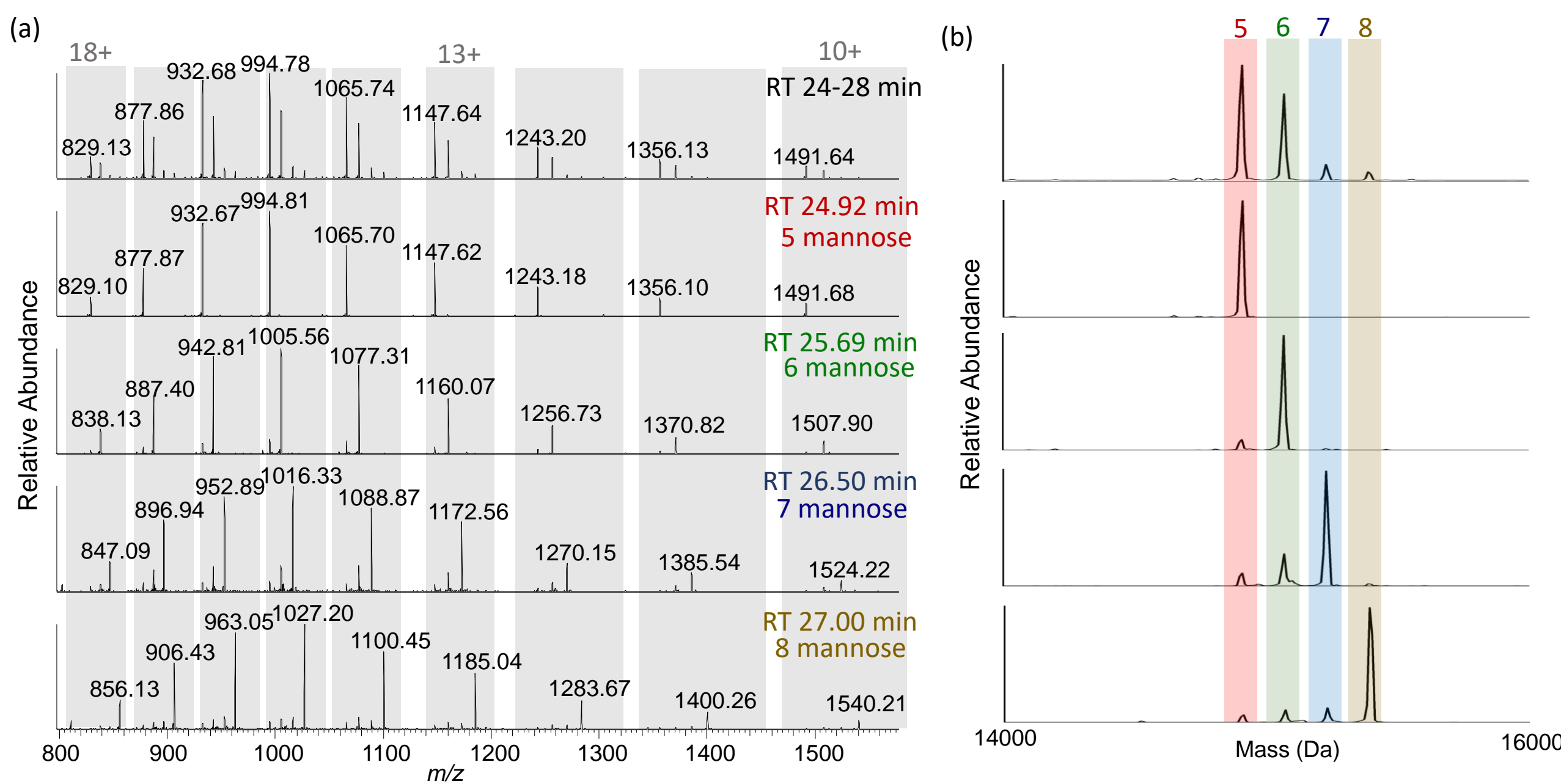


Figure S2. (a) Expanded view of the MS1 spectra of RNase B at each retention time shown in **Figure S1a**, and (b) the corresponding deconvoluted mass spectra where each color shaded region represents a different glycoform containing 5 to 8 mannoses as indicated by the number above the shaded regions.

(a) HCD: 39% coverage

```

N K[E T A A A K F E R]Q[H]M[D S S]T[S]A]A 20
21[S]S]S]N]Y C]N]Q]M]M]K]S]R]N]L]T]K]D]R]C 40
41 K P V N T F V H]E]S L A]D]V]Q]A]V C]S]Q 60
61[K]N]V]A]C]K]N]G]Q]T]N]C]Y]Q]S]Y]S]T]M]S 80
81 I T D C R E T G S S K Y]P]N]C]A]Y]K]T]T 100
101 Q A N K]H]I]I]V]A]C]E]G]N]P]Y]V]P]V]H]F 120
121]D]A]S]V]C

```

(b) ETD: 76% coverage

```

N K[E]T]A]A]A]A]K]F]E]R]Q]H]M]D]S]S]T]S]A]A 20
21[S]S]S]N]Y C]N]Q]M]M]K]S]R]N]L]T]K]D]R]C 40
41[K]P]V]N]T]F]V]H]E]S L]A]D]V]Q]A]V C]S]Q 60
61[K]N]V]A]C]K]N]G]Q]T]N]C]Y]Q]S]Y]S]T]M]S 80
81 I T D C R[E]T]G]S]S]K]Y]P]N]C]A]Y]K]T]T 100
101]Q]A]N]K]H]I]I]V]A]C]E]G]N]P]Y]V]P]V]H]F 120
121]D]A]S]V]C

```

(c) EThcD: 82% coverage

```

N K[E]T]A]A]A]A]K]F]E]R]Q]H]M]D]S]S]T]S]A]A 20
21[S]S]S]N]Y]C]N]Q]M]M]K]S]R]N]L]T]K]D]R]C 40
41[K]P]V]N]T]F]V]H]E]S L]A]D]V]Q]A]V]C]S]Q 60
61[K]N]V]A]C]K]N]G]Q]T]N]C]Y]Q]S]Y]S]T]M]S 80
81 I]T]D]C]R]E]T]G]S]S]K]Y]P]N]C]A]Y]K]T]T 100
101]Q]A]N]K]H]I]I]V]A]C]E]G]N]P]Y]V]P]V]H]F 120
121]D]A]S]V]C

```

(d) UVPD: 93% coverage

```

N K[E]T]A]A]A]A]K]F]E]R]Q]H]M]D]S]S]T]S]A]A 20
21[S]S]S]N]Y]C]N]Q]M]M]K]S]R]N]L]T]K]D]R]C 40
41[K]P]V]N]T]F]V]H]E]S L]A]D]V]Q]A]V]C]S]Q 60
61[K]N]V]A]C]K]N]G]Q]T]N]C]Y]Q]S]Y]S]T]M]S 80
81 I]T]D]C]R]E]T]G]S]S]K]Y]P]N]C]A]Y]K]T]T 100
101]Q]A]N]K]H]I]I]V]A]C]E]G]N]P]Y]V]P]V]H]F 120
121]D]A]S]V]C

```

■ a/x
■ b/y
■ c/z

Figure S3. Comparison of sequence maps derived from (a) HCD, (12 NCE), (b) ETD (14), (c) EThcD (10, 10 NCE), and (d) 193 nm UVPD UVPD (1 pulse, 2 mJ) of RNase B (15+) with one penta-mannose localized at Asn34 (site shaded in gold). The backbone cleavage sites are color-coded based on the types of fragment ions produced. Fragment ion identifications are given in **Table S8**.

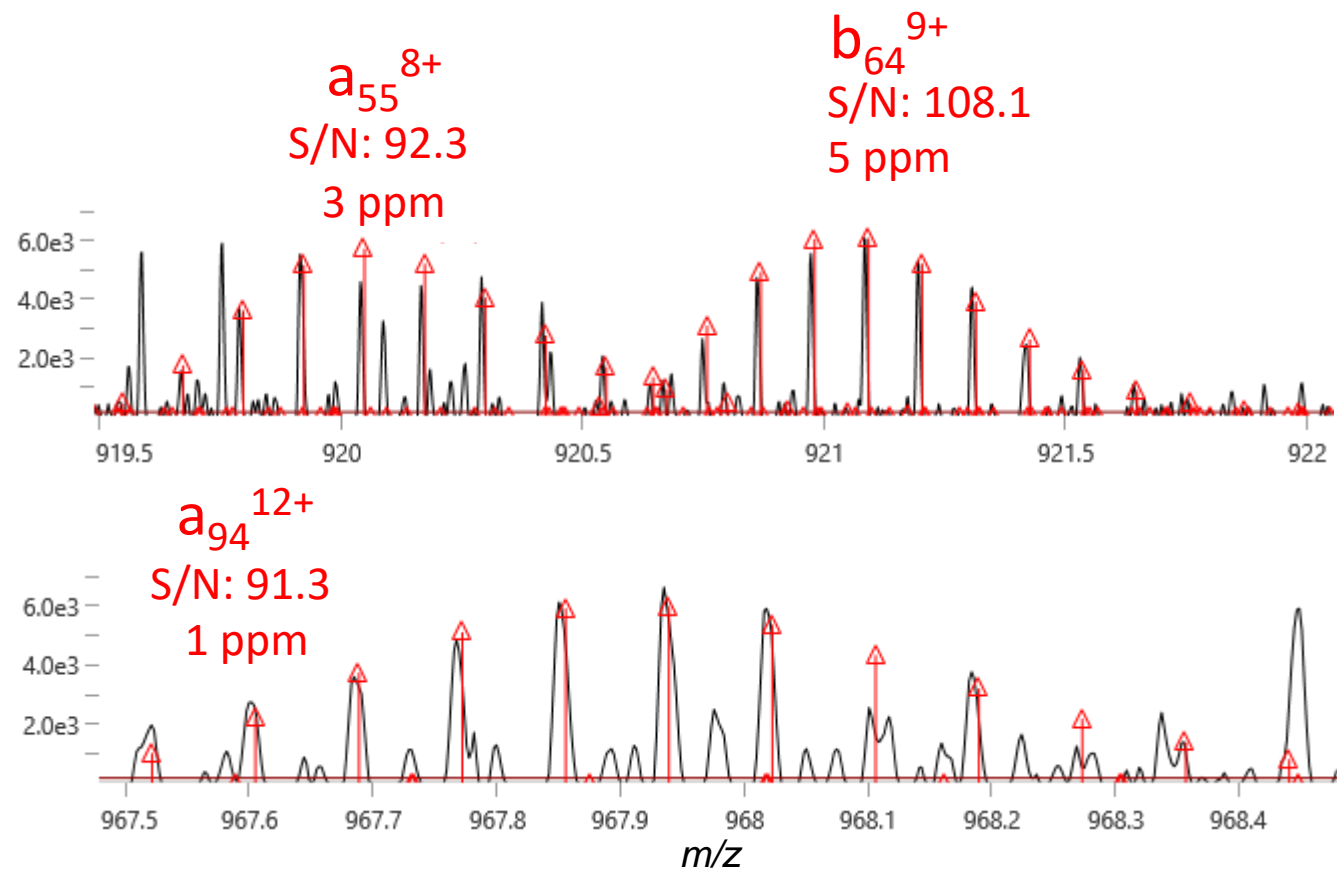
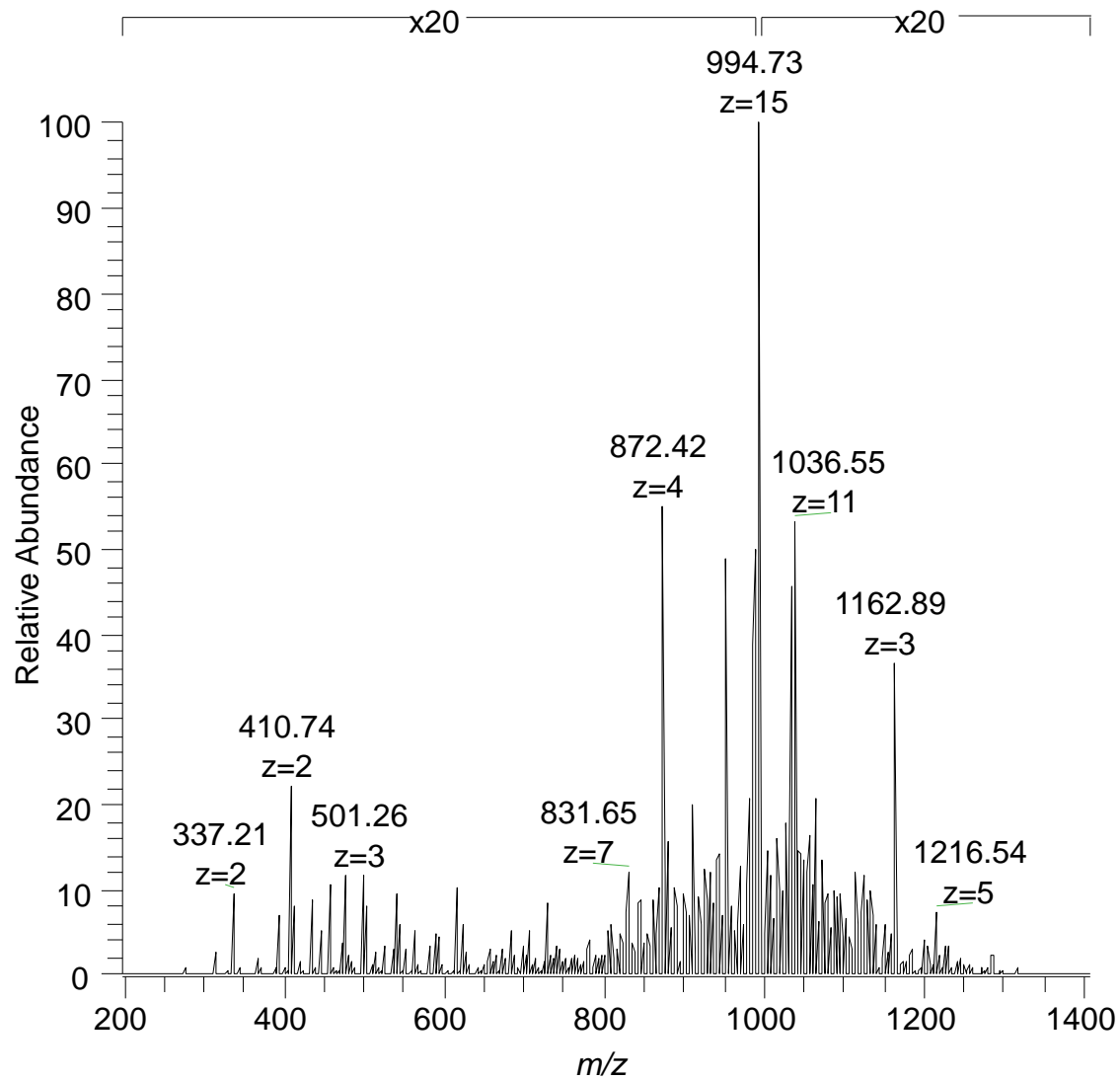


Figure S4. UVPD (1 pulse, 2 mJ) spectrum of RNase B with 5 mannoses, 15+ charge state, with expanded sections of the mass spectra on the right showing the experimental isotope patterns, theoretical isotopic fits, and mass errors for three fragment ions generated using TD validator.

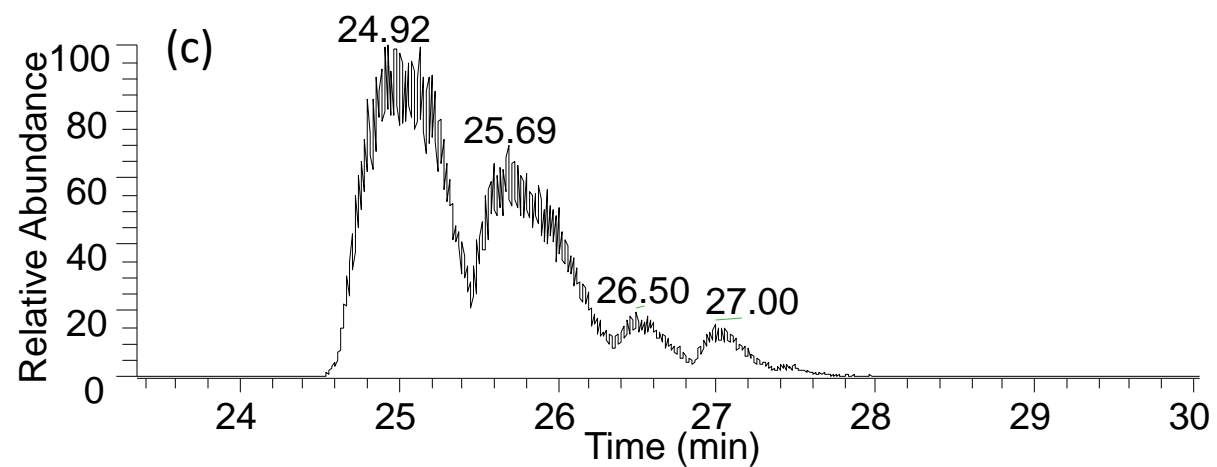
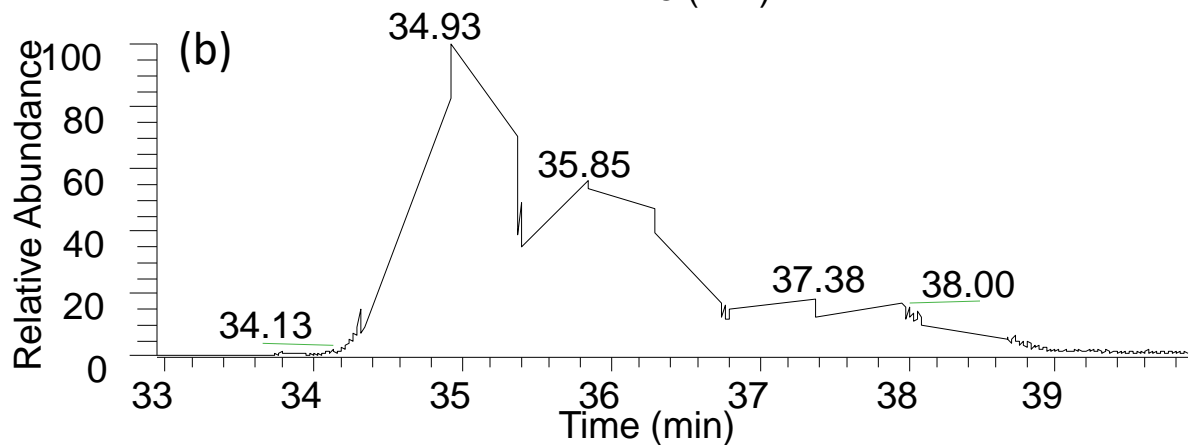
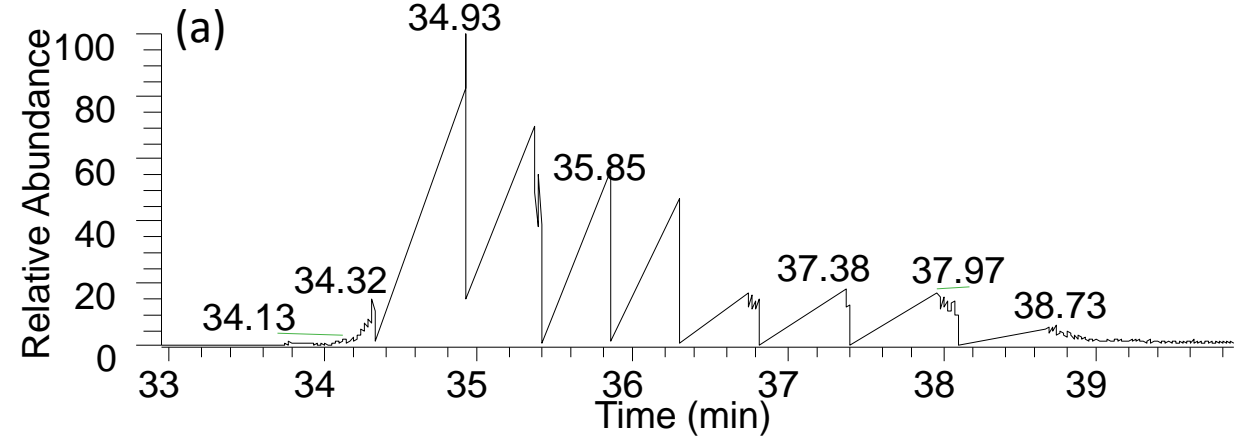


Figure S5. A comparison of peak shapes for runs of RNase B based on (a) both MS1 and UVPD scans included, (b) the same UVPD run with only MS1 scans retained in the chromatogram, and (c) MS1 scan only (UVPD not performed).

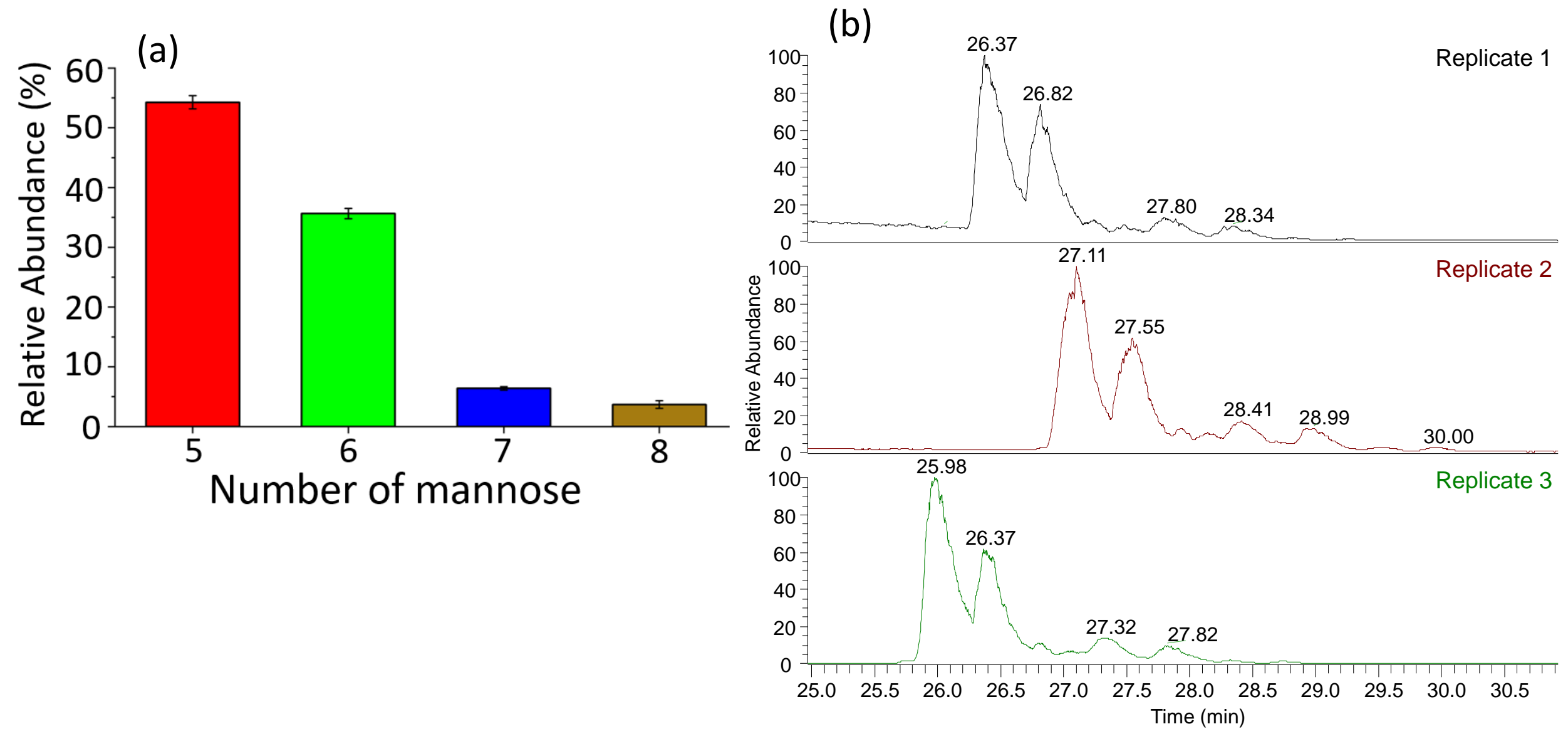


Figure S6. (a) Relative abundances of glycoforms of RNase B are compared with error bars representing the standard deviation based on three replicates and (b) chromatographic traces from three replicates. Peak areas vary little, but shifts in retention time are caused by different nanoESI emitters used to collect each replicate.

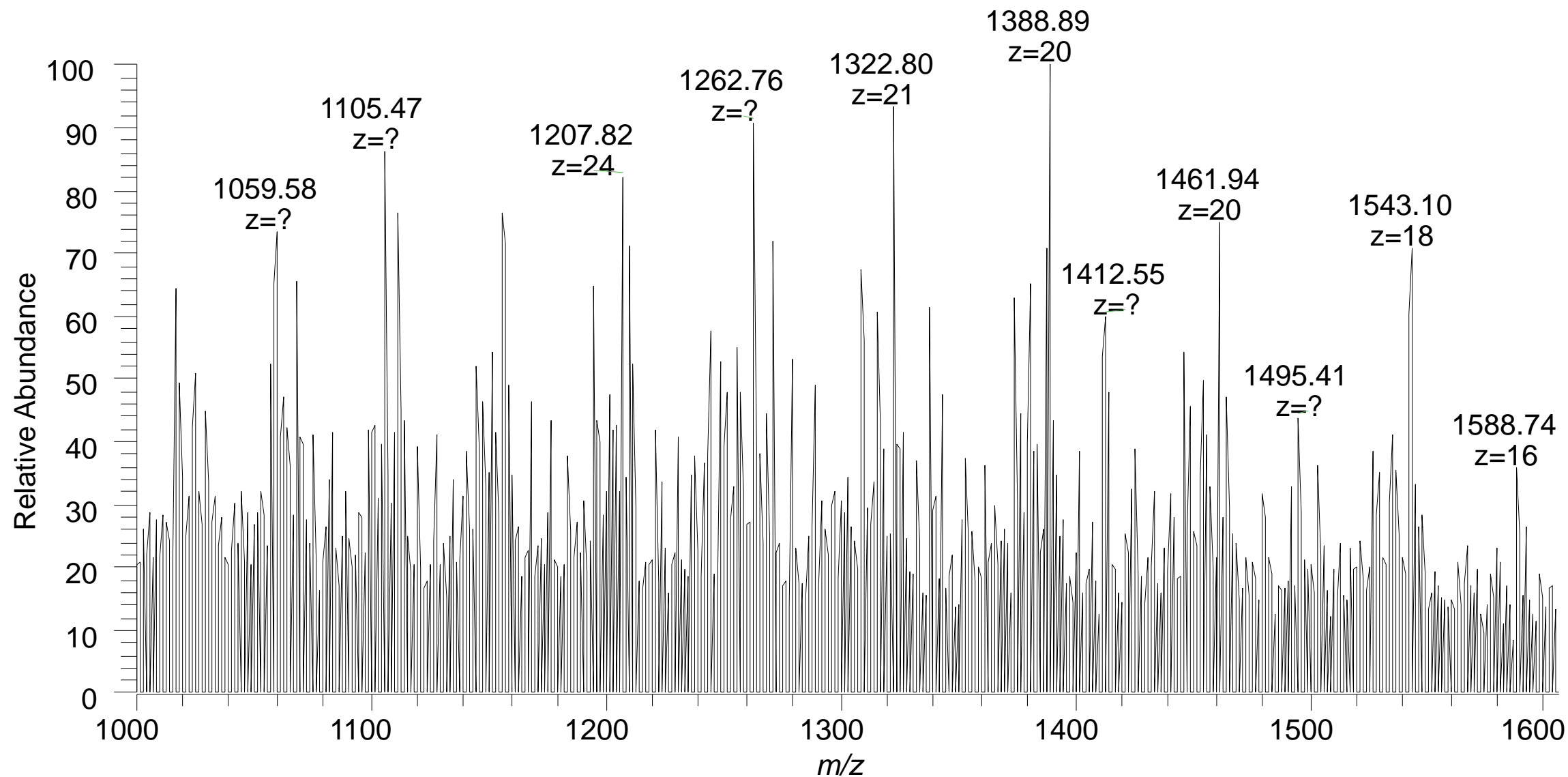


Figure S7. Expanded region of the high resolution MS1 spectrum of glycosylated HA via direct infusion showing overlapping charge states of various glycoforms and incorrect charge state assignments.

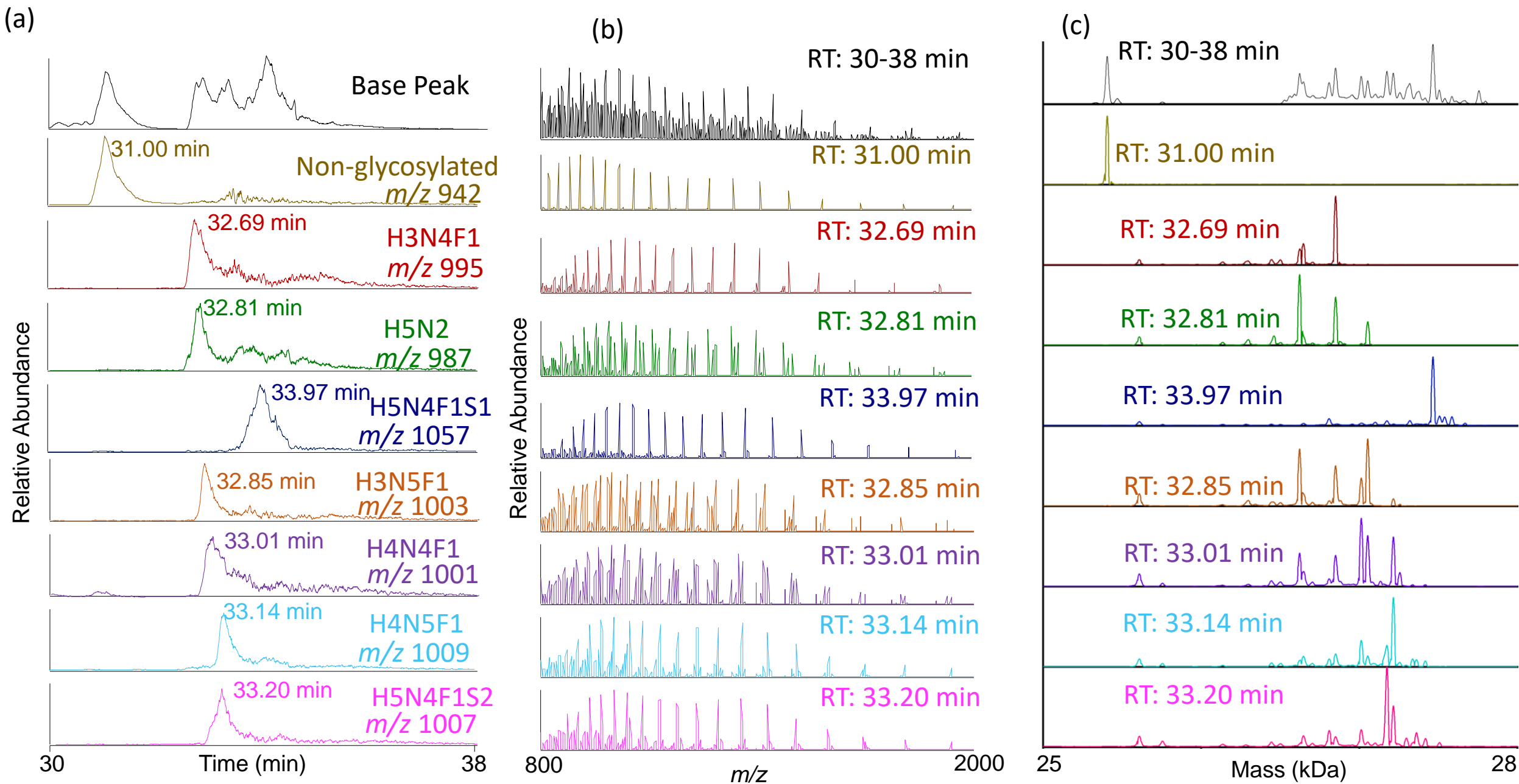


Figure S8. (a) Base peak and extracted ion chromatograms for the most abundant charge states of each glycoform of HA, (b) MS1 spectra corresponding to the retention time at the peak maximum, and (c) the corresponding deconvoluted mass spectra.

No glycan: 82%

H3N5F1: 67%

H5N4F1: 70%

H3N4F1: 74%

H4N4F1: 69%

H5N2: 72%

H4N5F1: 71%

■ a/x
 ■ b/y
 ■ c/z



Figure S9. Sequence coverage maps of additional HA glycoforms (26+ charge state) derived from UVPD (1 pulse, 2 mJ). The glycosylation site is shaded in gold (N40). These maps correspond to results reported in **Figure 1**. The backbone cleavage sites are color-coded based on the types of fragment ions produced. Fragment ion identifications are given in **Table S8**.

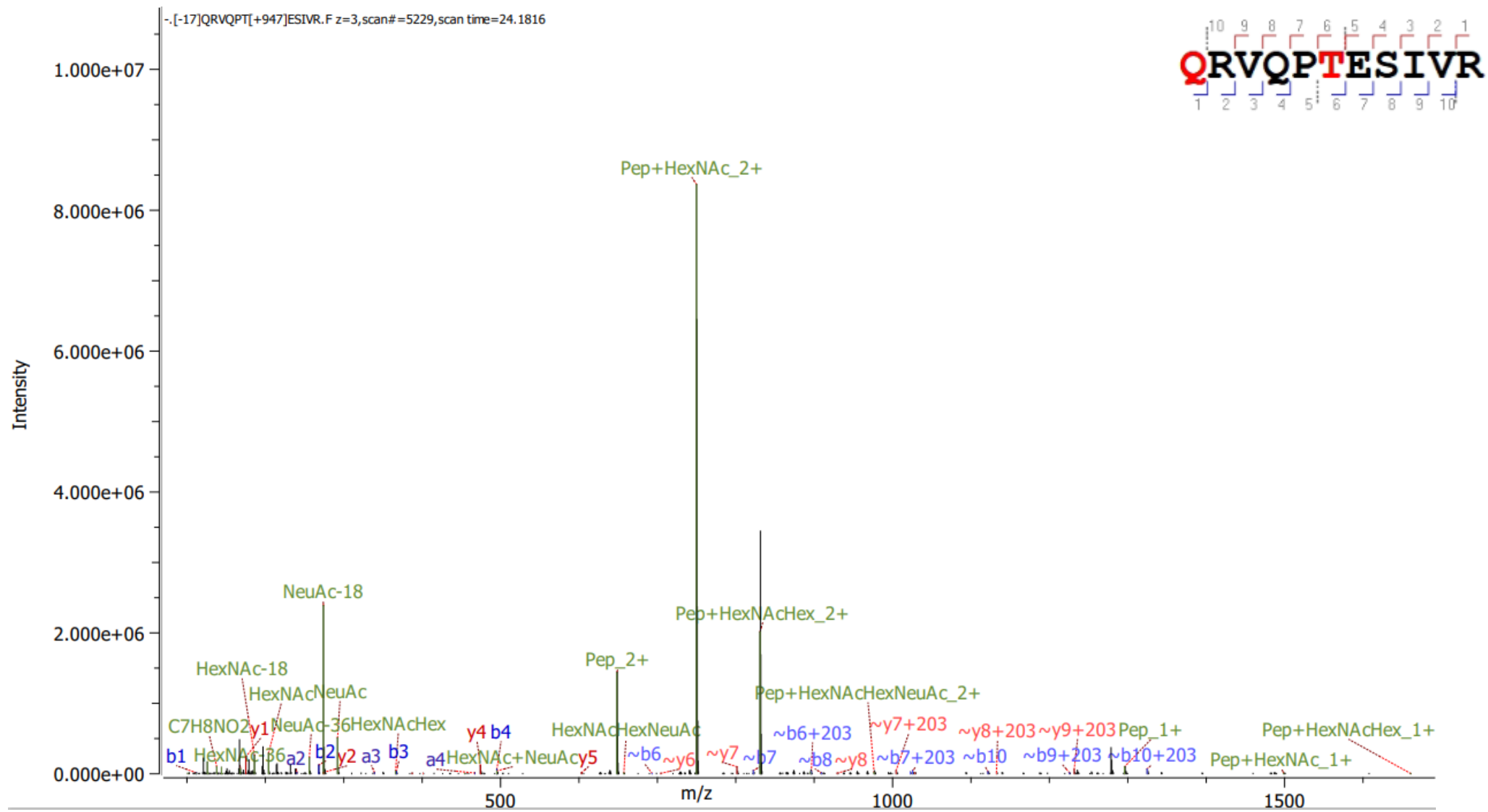


Figure S10. HCD (30 NCE) spectrum of a tryptic peptide (m/z 749.90, 2+ charge state) of WT RBD confirming the addition of pyroGlu to the N terminus.

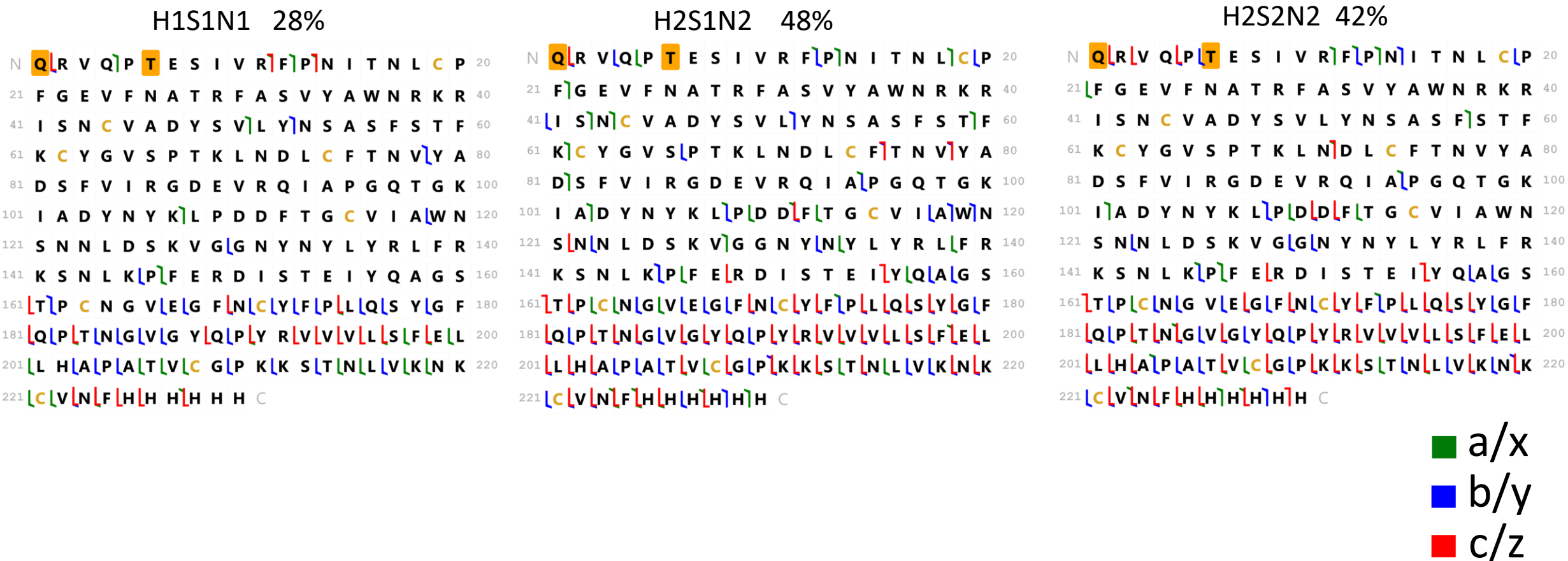


Figure S11. Sequence coverage maps generated from UVPD fragment (1 pulse, 2 mJ of the 26+ charge state) of additional WT RBD glycoforms with sequence coverages listed. The sites with modifications are shaded in gold. The glycan is attached to T6, and the other modification corresponds to the addition of pyroGlu (+111 Da) at the N terminus. The backbone cleavage sites are color-coded based on the types of fragment ions produced. Fragment ion identifications are given in **Table S8**.

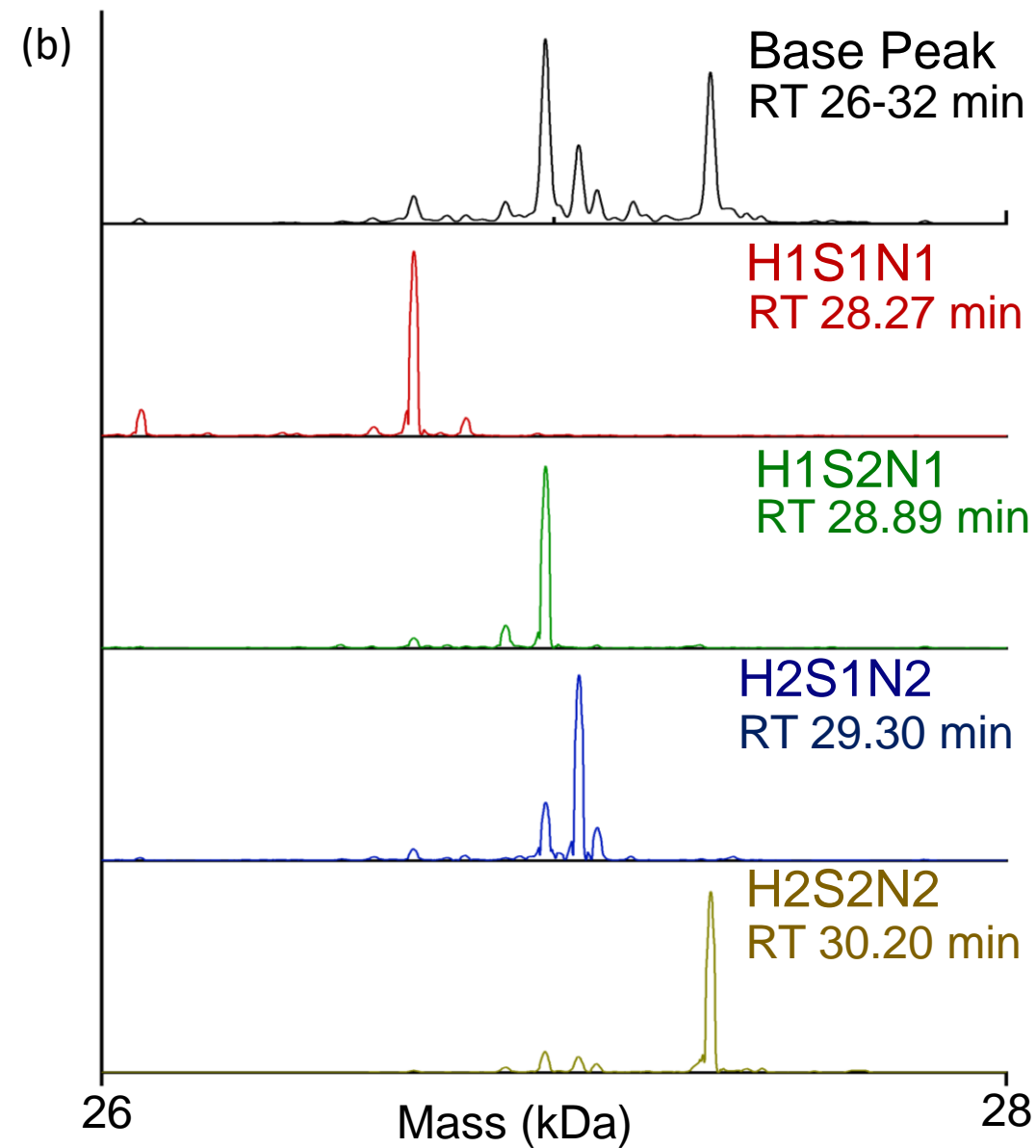
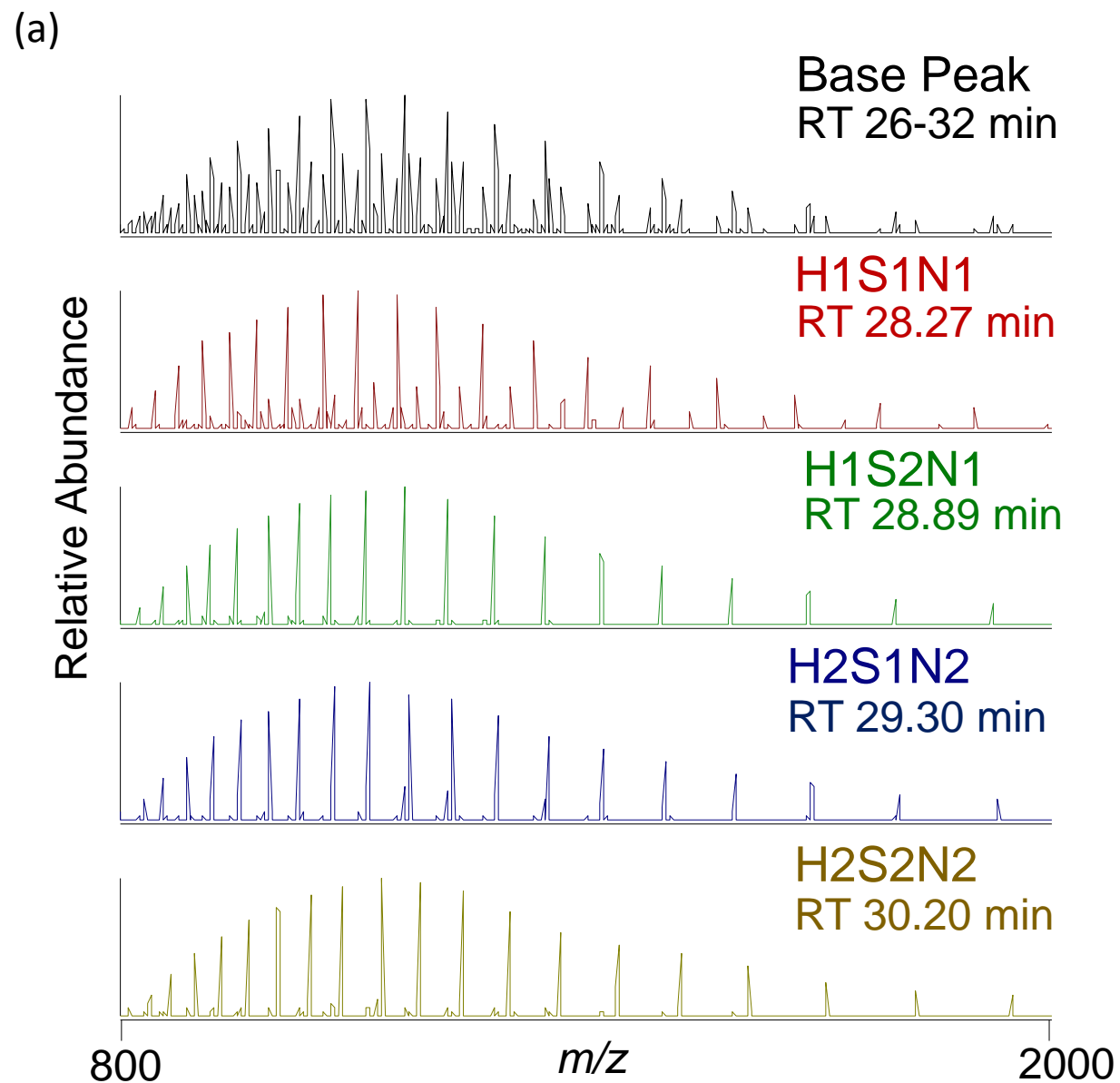


Figure S12. (a) MS1 spectra corresponding to the retention time of each glycoform of the WT RBD shown in **Figure 2a**; these are expanded spectra compared to the truncated ones shown in **Figure 2b**, and (b) the corresponding deconvoluted mass spectra.

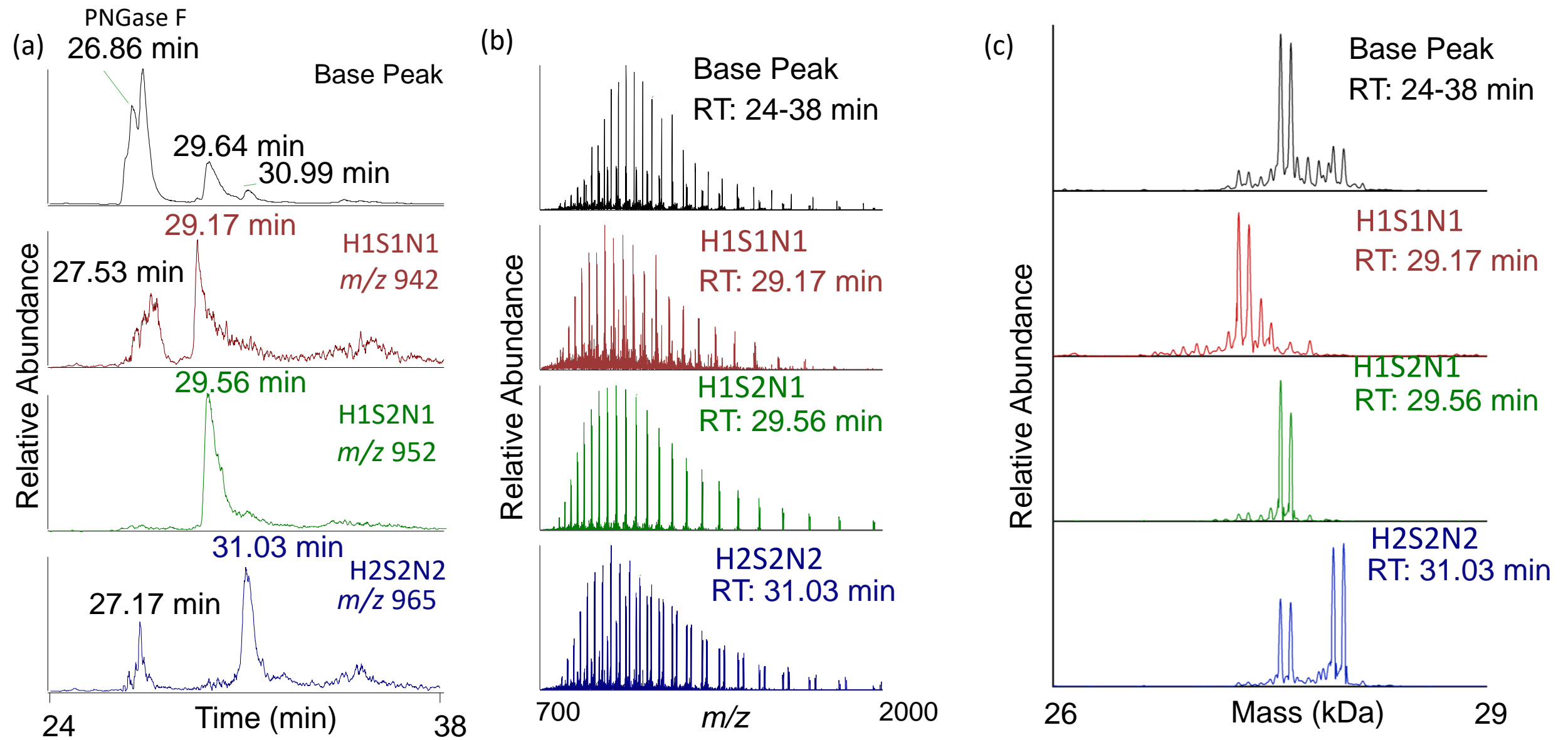


Figure S13. (a) Base peak chromatogram and EICs for the most abundant charge states of each O-glycoform of K417N/E484K/N501Y RBD, (b) MS1 spectra corresponding to the retention time at the peak maximum, and (c) the corresponding deconvoluted mass spectra with average intact masses given in **Table S11**.

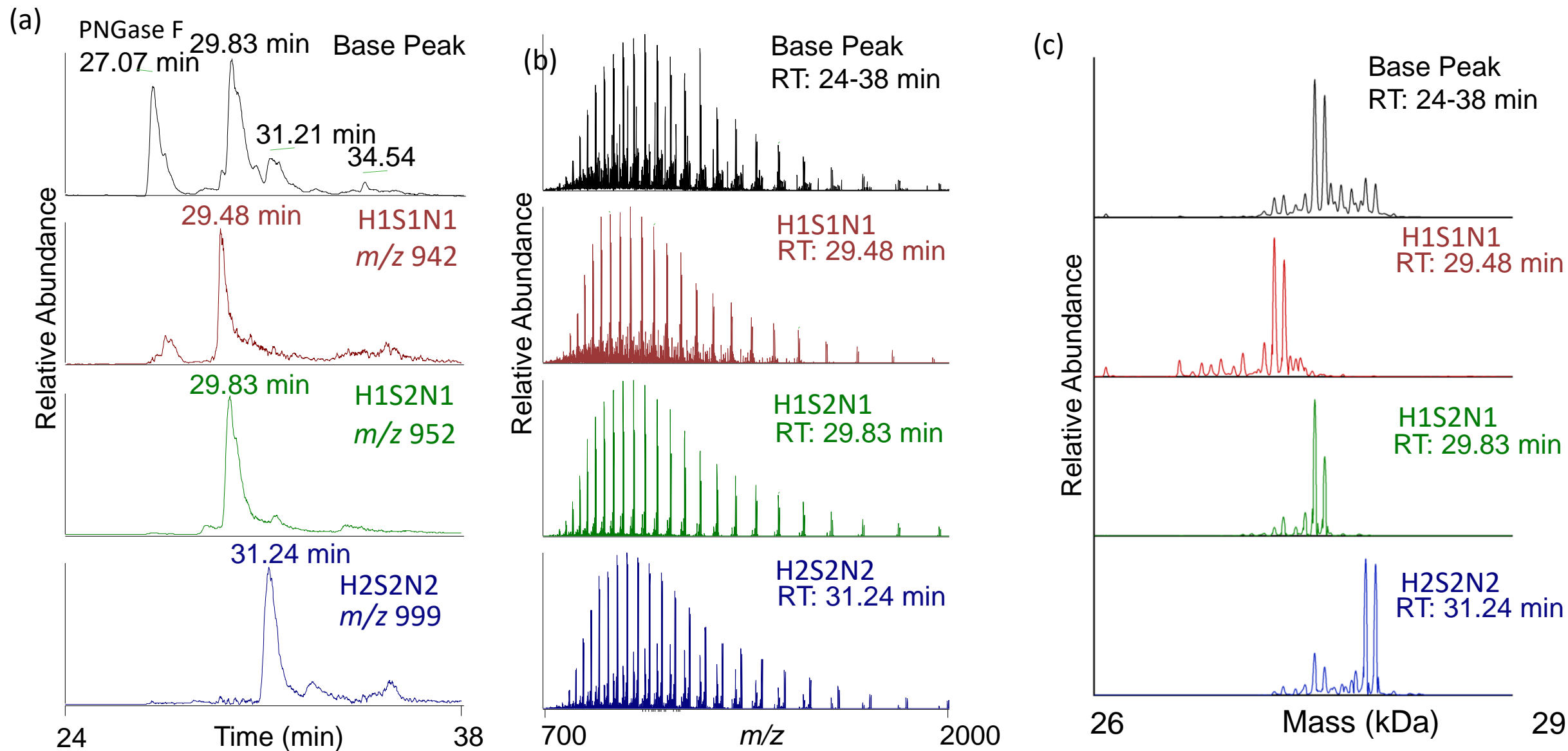


Figure S14. (a) Base peak chromatogram and EICs for the most abundant charge states of each L452R RBD O-glycoform, (b) MS1 spectra corresponding to the retention time at the peak maximum, and (c) the corresponding deconvoluted mass spectra with average intact masses given in **Table S11**.

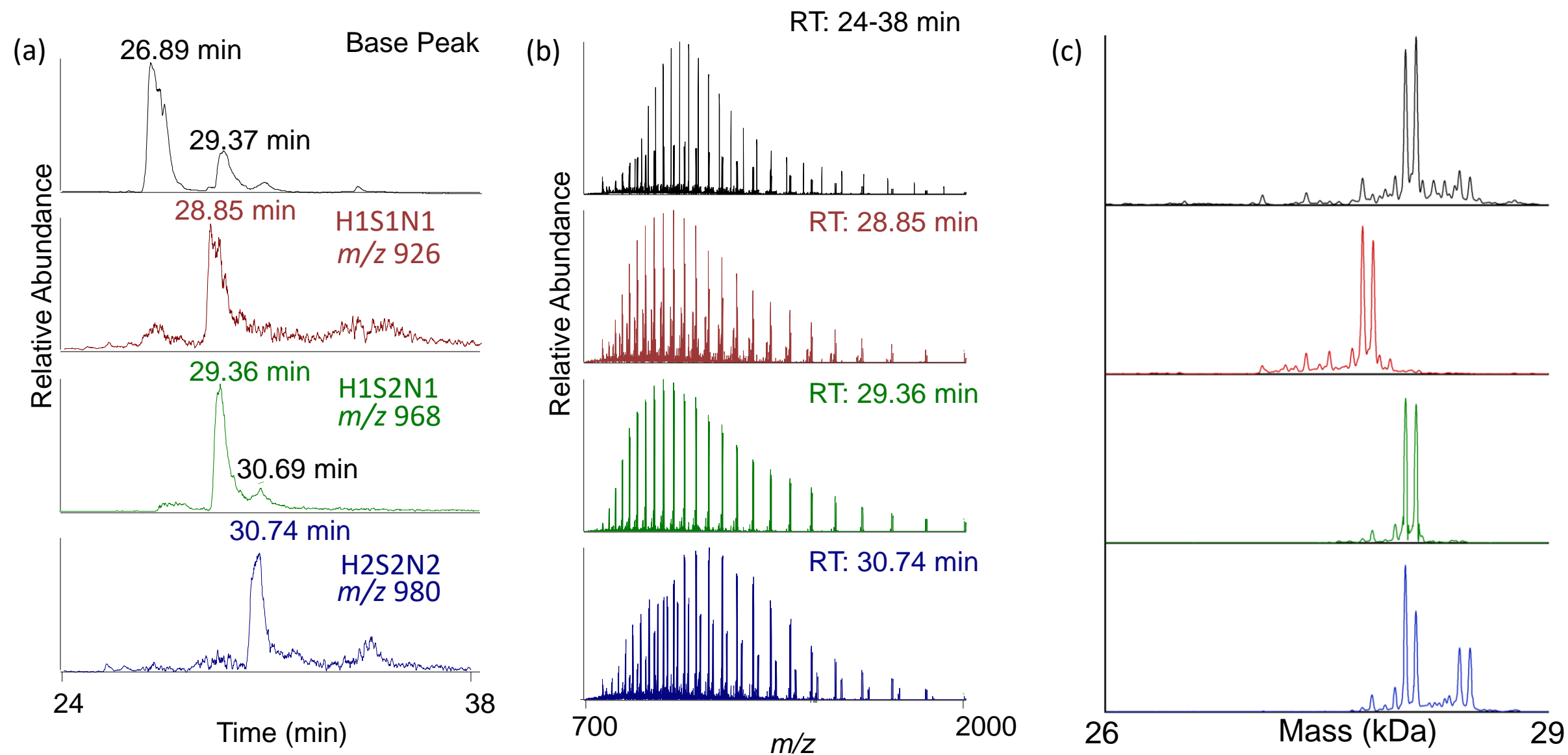


Figure S15. (a) Base peak chromatogram and EICs for the most abundant charge states of each G476S RBD O-glycoform, (b) MS1 spectra corresponding to the retention time at the peak maximum, and (c) the corresponding deconvoluted mass spectra with average intact masses given in **Table S11**.

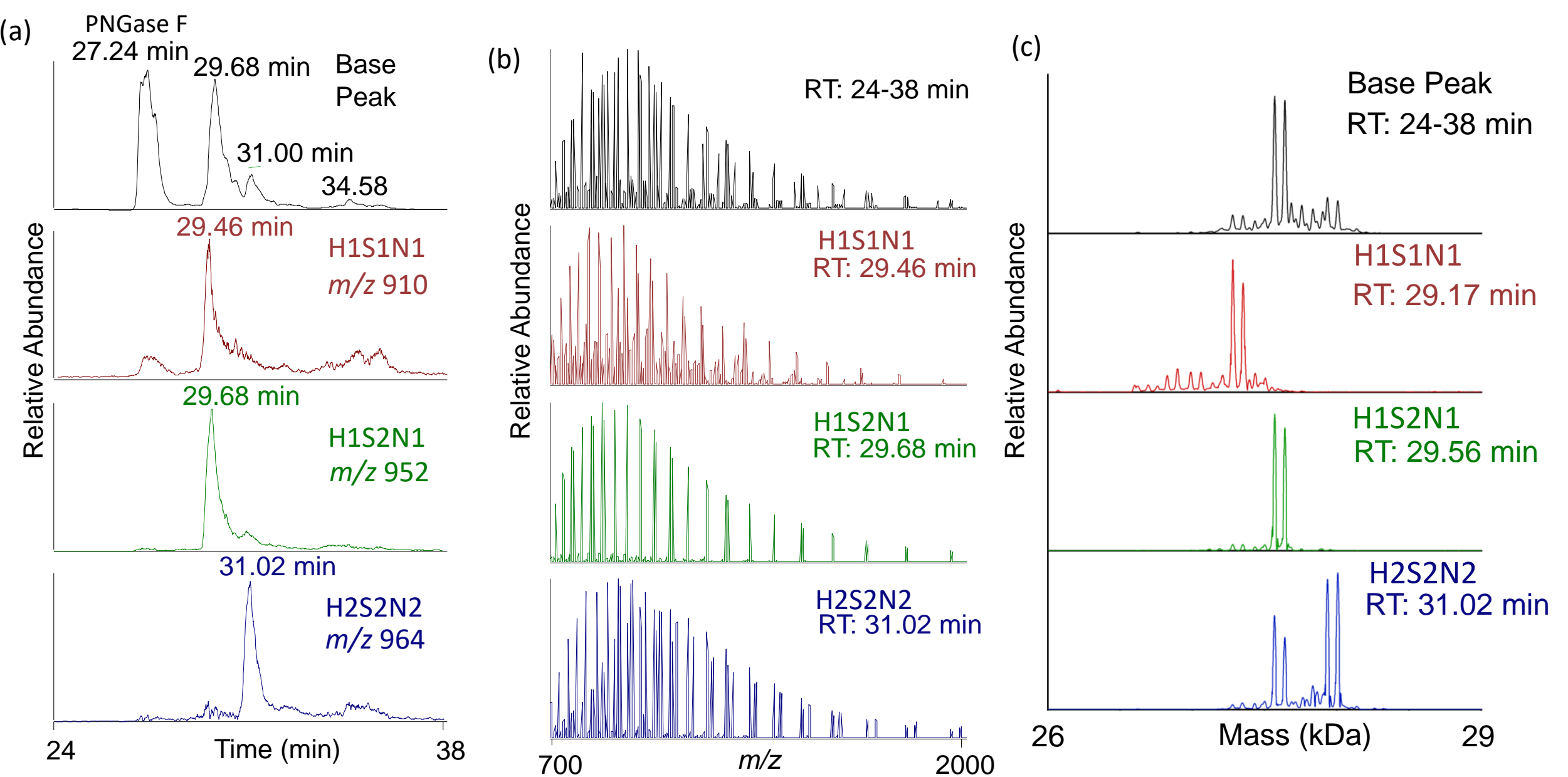


Figure S16. (a) Base peak chromatogram and EICs for the most abundant charge states of each A475V RBD O-glycoform, (b) MS1 spectra corresponding to the retention time at the peak maximum, and (c) the corresponding deconvoluted mass spectra with average intact masses given in **Table S11**.

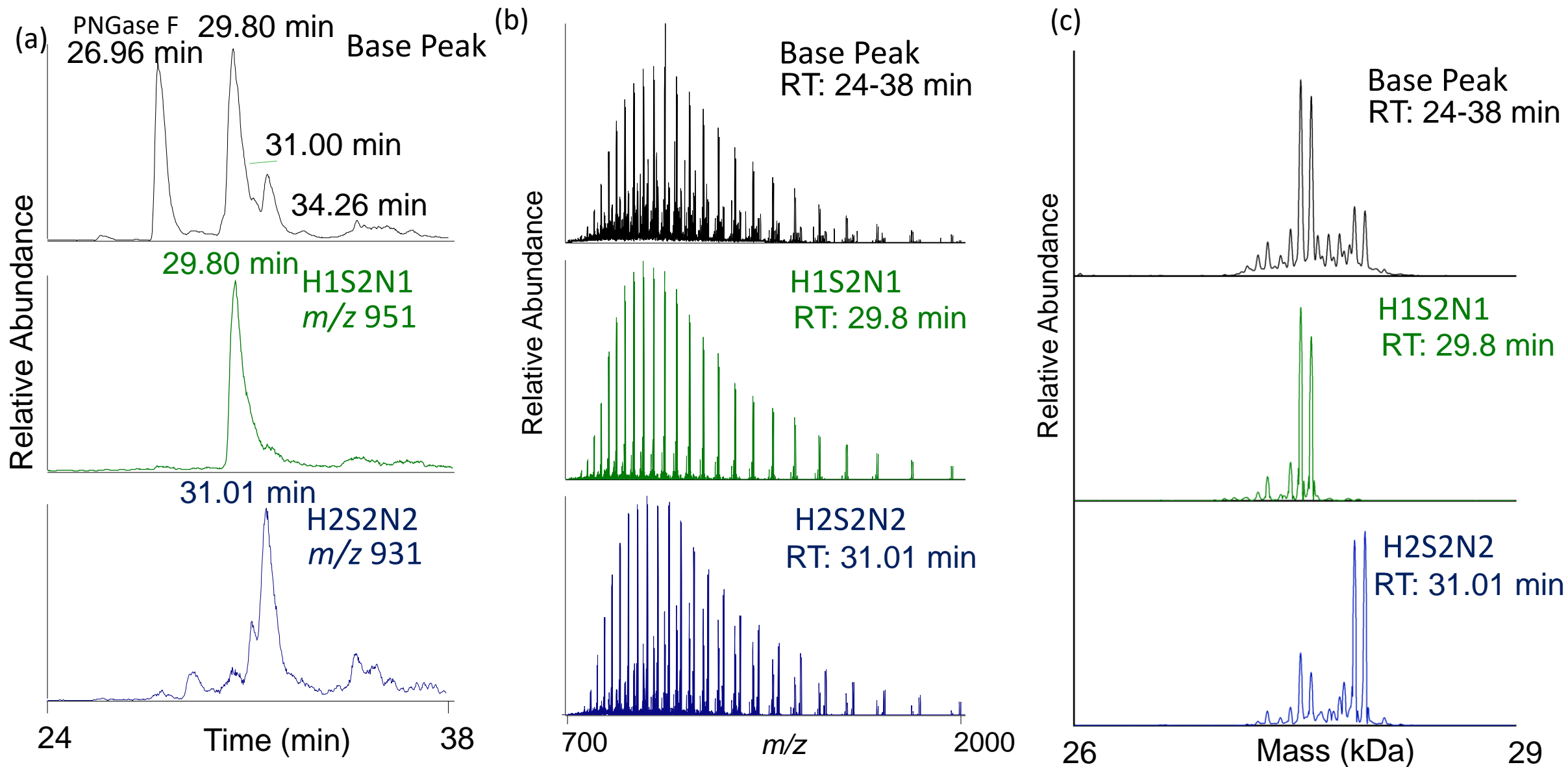


Figure S17. (a) Base peak chromatogram and EICs for the most abundant charge states of each E484K RBD O-glycoform, (b) MS1 spectra corresponding to the retention time at the peak maximum, and (c) the corresponding deconvoluted mass spectra with average intact masses given in **Table S11**.

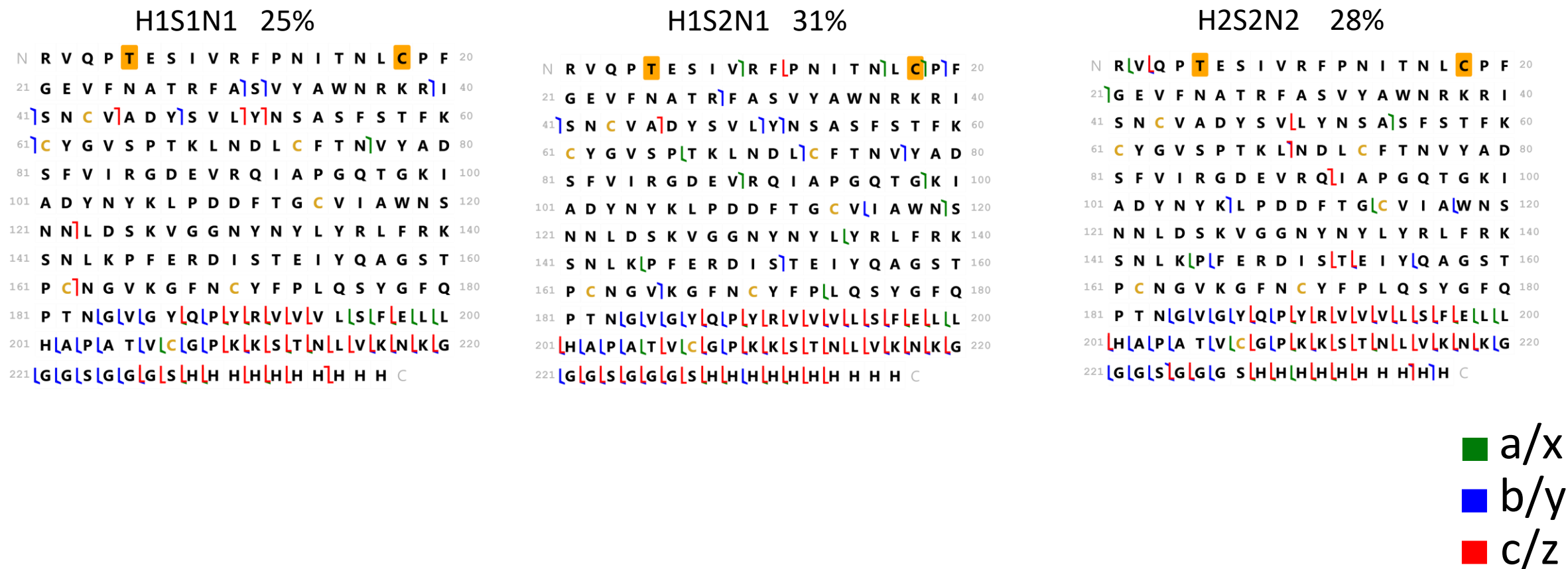


Figure S18. Sequence maps of each O-glycoform of K417N/E484K/N501Y RBD based on UVPD (1 pulse, 2 mJ). The sites of modification are shaded in gold. Modification at T5 represents the glycan listed above each map, and the modification at C18 represents Cys alkylation by dimethylaminoethyl halide. The backbone cleavage sites are color-coded based on the types of fragment ions produced. Fragment ion identifications are given in **Table S8**.

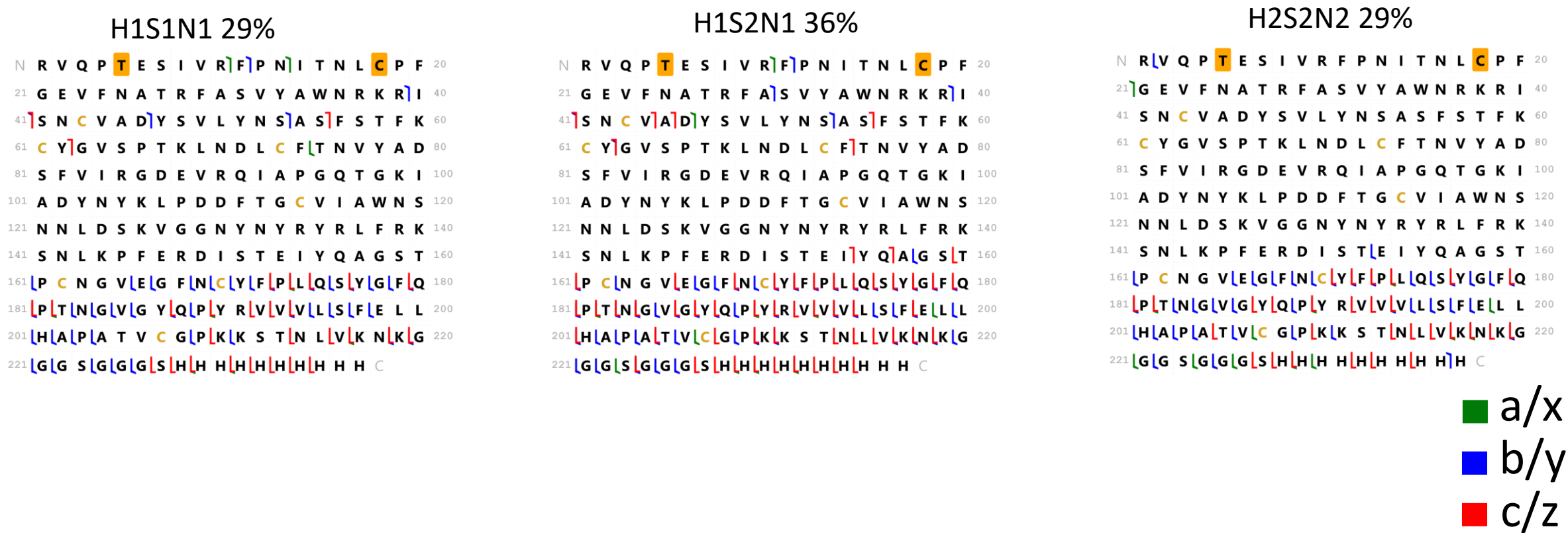


Figure S19. Sequence maps of each O-glycoform of L452R RBD based on UVPD (1 pulse, 2 mJ). Modification sites are shaded in gold. Modification at T5 represents the glycan listed above each map, and the modification at C18 represents Cys alkylation by dimethylaminoethyl halide. The backbone cleavage sites are color-coded based on the types of fragment ions produced. Fragment ion identifications are given in **Table S8**.

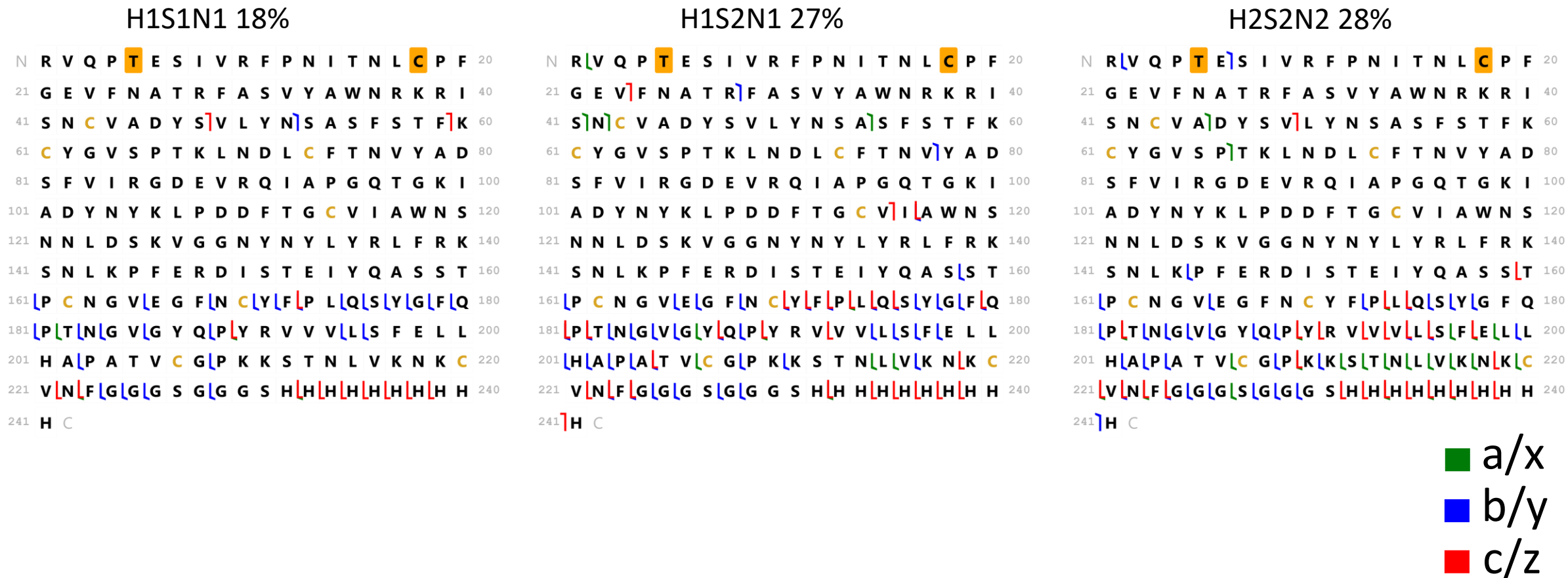


Figure S20. Sequence maps of each O-glycoform of G476S RBD based on UVPD (1 pulse, 2 mJ). Modification sites are shaded in gold. Modification at T5 represents the glycan listed above each map, and the modification at C18 represents Cys alkylation by dimethylaminoethyl halide. The backbone cleavage sites are color-coded based on the types of fragment ions produced. Fragment ion identifications are given in **Table S8**.

H1S1N1 24%

```

N R V Q P T E S I V R F P N I T N L C P F 20
21 G E V F N A T R F A S V Y A W N R K R I 40
41 S N C V A D Y S V L Y N S A S F S T F K 60
61 C Y G V S P T K L N D L C F T N V Y A D 80
81 S F V I R G D E V R Q I A P G Q T G K I 100
101 A D Y N Y K L P D D F T G C V I A W N S 120
121 N N L D S K V G G N Y N Y L Y R L F R K 140
141 S N L K P F E R D I S T E I Y Q V G S T 160
161 P C N G V E G F N C Y F P L L Q S Y G F L Q 180
181 P T N G V G Y Q P Y R V V V L S F E L L L 200
201 H A P A T V C G P K K S T N L L V K N K L G 220
221 G G S G G G S H H H H H H H H H H H C
  
```

H1S2N1 54%

```

N R V Q P T E S I V R F P N I T N L C P F 20
21 G E V F N A T R F A S V Y A W N R K R I 40
41 S N C V A D Y S V L Y N S A S F S T F K 60
61 C Y G V S P T K L N D L C F T N V Y A D 80
81 S F V I R G D E V R Q I A P G Q T G K I 100
101 A D Y N Y K L P D D F T G C V I A W N S 120
121 N N L D S K V G G N Y N Y L Y R L F R K 140
141 S N L K P F E R D I S T E I Y Q V G S T 160
161 P C N G V E G F N C Y F P L L Q S Y G F L Q 180
181 P T N G V G Y Q P Y R V V V L S F E L L L 200
201 H A P A T V C G P K K S T N L L V K N K L G 220
221 G G S G G G S H H H H H H H H H H H C
  
```

H2S2N2 40%

```

N R V Q P T E S I V R F P N I T N L C P F 20
21 G E V F N A T R F A S V Y A W N R K R I 40
41 S N C V A D Y S V L Y N S A S F S T F K 60
61 C Y G V S P T K L N D L C F T N V Y A D 80
81 S F V I R G D E V R Q I A P G Q T G K I 100
101 A D Y N Y K L P D D F T G C V I A W N S 120
121 N N L D S K V G G N Y N Y L Y R L F R K 140
141 S N L K P F E R D I S T E I Y Q V G S T 160
161 P C N G V E G F N C Y F P L L Q S Y G F L Q 180
181 P T N G V G Y Q P Y R V V V L S F E L L L 200
201 H A P A T V C G P K K S T N L L V K N K L G 220
221 G G S G G G S H H H H H H H H H H H C
  
```

■ a/x
■ b/y
■ c/z

Figure S21. Sequence maps of each O-glycoform of A475V RBD based on UVPD (1 pulse, 2 mJ). Modification sites are shaded in gold. Modification at T5 represents the glycan listed above each map, and the modification at C18 represents Cys alkylation by dimethylaminoethyl halide. The backbone cleavage sites are color-coded based on the types of fragment ions produced. Fragment ion identifications are given in **Table S8**.

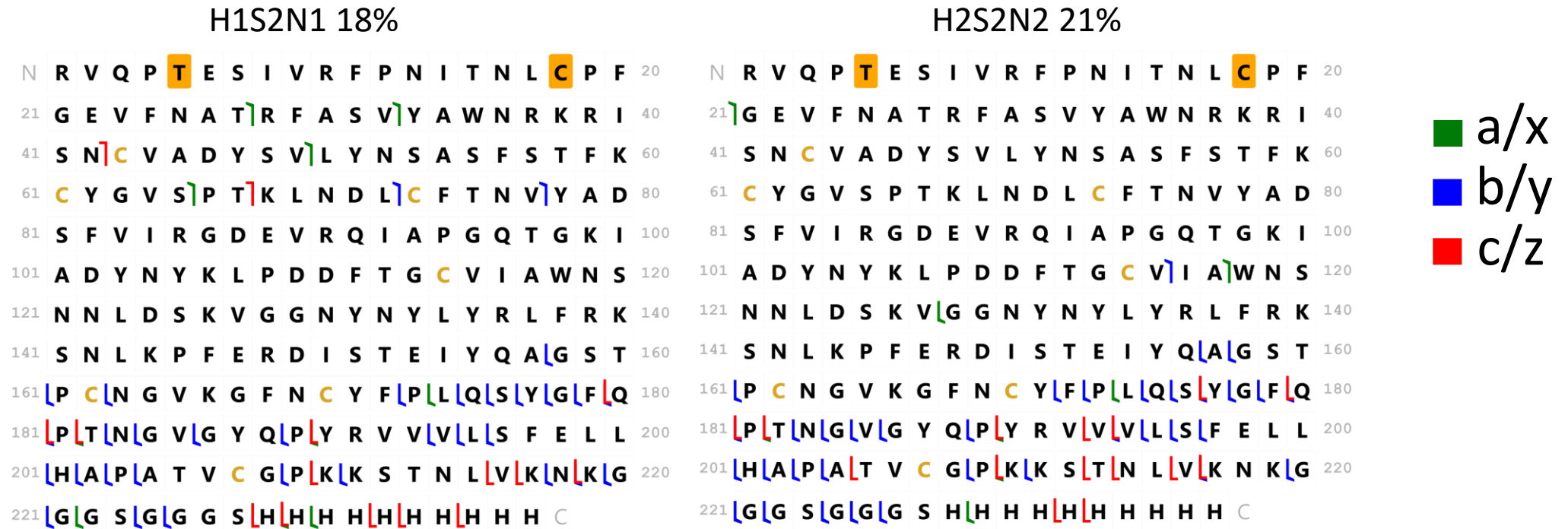


Figure S22. Sequence maps of each O-glycoform of E484K RBD based on UVPD (1 pulse, 2 mJ). Modification sites are shaded in gold. Modification at T5 represents the glycan listed above each map, and the modification at C18 represents Cys alkylation by dimethylaminoethyl halide. The backbone cleavage sites are color-coded based on the types of fragment ions produced. Fragment ion identifications are given in **Table S8**.